Environmental Science & Technology

pubs.acs.org/est

Article

Mineral Dynamics Revealed by Fe^{2+}-Catalyzed Recrystallization of U-Incorporated Goethite

Qingyin Xia, Prachi Joshi, Zezhen Pan,* Marina Lazarov, Barbora Bartova, Xiyang Xu, Tim Prüssmann, Andreas Kappler, Hailiang Dong,* Stefan Weyer, and Rizlan Bernier-Latmani*

Cite This: https://doi.org/10.1021/acs.est.5c11748

Read Online

ACCESS | Metrics & More | Article Recommendations | Supporting Information

ABSTRACT: Iron (oxyhydr)oxides are capable of structurally incorporating and releasing trace elements through Fe^{2+}-induced recrystallization. However, estimation of the extent of recrystallization varies among studies using isotopic tracers and those examining the release of occluded trace elements. To provide further insight into the dynamics of Fe^{2+}-catalyzed iron (oxyhydr)oxide recrystallization, and to accurately interpret the isotopic and elemental compositions of iron (oxyhydr)oxides in the rock record, we probed the coupled dynamics of goethite isotopic exchange and trace element cycling during Fe^{2+}-induced recrystallization. Herein, ^{57}Fe labeled Fe^{2+} was reacted with U(V)-incorporated goethite, and the resulting isotopic and elemental interactions were systematically characterized and modeled. Partial release of incorporated U (3.9%) was observed, which suggested limited recrystallization while Fe isotope measurements suggested nearly complete isotopic mixing after 30 days. A box model incorporating partial and gradual back-reaction estimated an overall goethite recrystallization extent of ~32.8%, narrowing the gap to the observed U release (3.9%) as compared to the traditional fast back-reaction-only model (88%). This study highlights the role of Fe^{2+}-driven recrystallization in controlling trace metal cycling and provides insights into the stability and reactivity of U-incorporated goethite in reducing environments. The findings refine our understanding of iron (oxyhydr)oxide recrystallization processes and their implications for trace element mobility in natural systems.

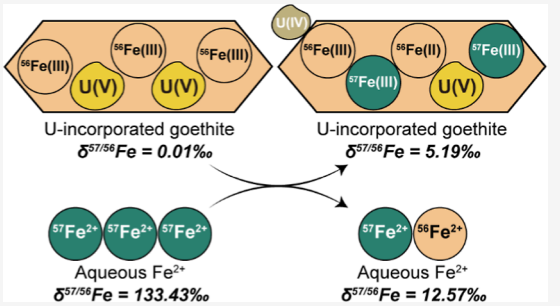

KEYWORDS: *mineral dynamics, Fe^{2+}-catalyzed recrystallization, iron (oxyhydr)oxides, U-incorporated goethite, partial and gradual back-reaction, box model*

INTRODUCTION

Iron (oxyhydr)oxides are widespread in nature. Their mineralogy is highly dynamic, resulting in the common presence of trace elements, including Al, Cr, Mn, Co, Ni, Cu, Zn, Sn and U.[1−8] For instance, trace elements can substitute for octahedrally coordinated Fe, during the Fe^{2+}-catalyzed transformation of amorphous or nanocrystalline ferrihydrite to more crystalline phases, e.g., goethite, lepidocrocite, magnetite and hematite.[7−10]

Fe^{2+}-catalyzed recrystallization has been proposed as a mechanism for the structural incorporation and release of trace metals in iron (oxyhydr)oxides.[11−16] For poorly crystalline Fe(III) (oxyhydr)oxides (e.g., ferrihydrite), this involves electron transfer and atom exchange between aqueous Fe^{2+} and surface Fe(III),[1−4] which results in the formation of more thermodynamically stable minerals such as goethite. In contrast, aqueous Fe^{2+} does not induce any noticeable secondary mineralization in stable iron (oxyhydr)oxides, as evidenced by no apparent variation in solution chemistry, mineral structure, or morphology.[17−20] Nonetheless, complex and dynamic reactions between aqueous Fe^{2+} and stable iron (oxyhydr)oxides were previously demonstrated through Fe isotope tracer studies.[17−22] Pedersen et al. (2005)[21] first demonstrated the release of ^{55}Fe from ^{55}Fe-labeled goethite after reaction with aqueous Fe^{2+} for 15 days.

A conceptual redox-driven conveyor belt model[17,18] was proposed to explain extensive Fe atom exchange in the absence of mineral phase transformation or morphology change. It invokes oxidative Fe^{2+} uptake and reductive Fe(III) dissolution occurring at distinct crystallographic faces, linked by electron conduction through the bulk structure. The model is supported by experimental observations and modeling results for hematite (α-Fe_2O_3) showing that Fe^{2+} preferentially sorbs to the (001) face and is further oxidized, whereas reductive dissolution occurs at the (hk0) face.[23,24]

However, quantifying the extent of Fe^{2+}-catalyzed recrystallization remains challenging,[17−19,25] despite its importance in

Received: August 24, 2025
Revised: November 24, 2025
Accepted: November 25, 2025

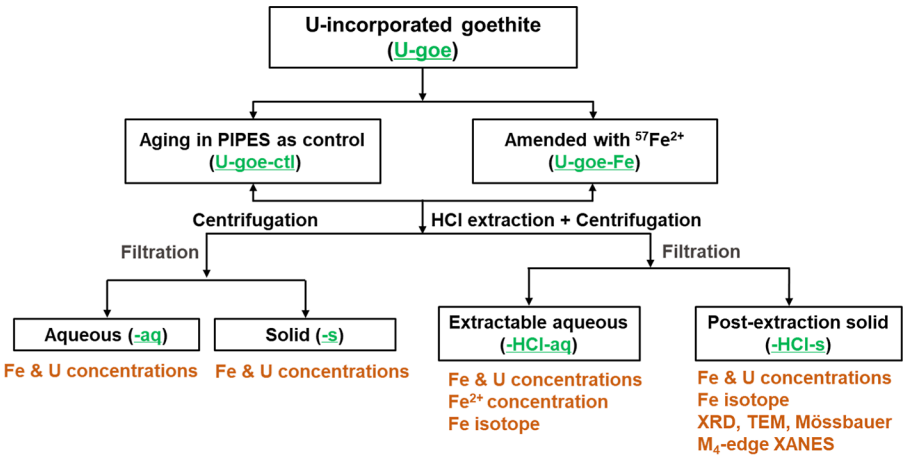

Figure 1. Schematic of experimental manipulations including the sample separation procedures. U-incorporated goethite (U-goe) is obtained after extraction of the ferrihydrite-transformation system with 0.5 M HCl for 36 h. Suspension of U-incorporated goethite w/o $^{57}Fe^{2+}$ was directly centrifuged and filtered to separate the aqueous phase (U-goe-Fe/ctl-aq) and solid pellet (U-goe-Fe/ctl-s). Identical suspension of U-incorporated goethite w/o $^{57}Fe^{2+}$ was equilibrated with HCl solution at a final concentration 0.5 M for 30 min to separate the acid extractable fraction (U-goe-Fe/ctl-HCl-aq) from the bulk goethite (U-goe-Fe/ctl-HCl-s).

interpreting the isotopic and elemental composition of iron (oxyhydr)oxides in the rock record. One major obstacle is the limited understanding of the extent of further dissolution-reprecipitation and associated atom exchange between solution and the recrystallized solid (referred to here as "back-reaction").[19,25,26] Most previous studies[17,18,27] have assumed that the back-reaction is instantaneous, complete, and involves the entire recrystallized solid. That is, every Fe atom in the recrystallized solid could back-react instantaneously and continuously with aqueous Fe^{2+}, resulting in isotopically homogeneous iron (oxyhydr)oxides, in isotopic equilibrium with aqueous Fe^{2+}. Consequently, extensive recrystallization was predicted for goethite (60−100%) over weeks.[17,18,27] However, recent studies postulated that the back-reaction between recrystallized goethite and Fe^{2+} is partial and gradual,[28−31] i.e., the recrystallized solid back-reacts over a continuum of time scales. Therefore, there will be a distribution of heterogeneous isotopic compositions within the bulk mineral. A model based on this assumption reported substantially lower recrystallization extents of goethite (14.1−19.8%).[19,25] Thus, the same isotopic data can be interpreted to yield different estimations of the extents of recrystallization.[17−19,25,27] At present, there is no satisfactory consensus for modeling iron (oxyhydr)oxides recrystallization.

In addition, cycling of trace elements between solid-phase iron (oxyhydr)oxides and solution is observed during Fe^{2+}-catalyzed iron (oxyhydr)oxides recrystallization,[1−4] providing a potential proxy to decipher iron (oxyhydr)oxides dynamics. Studies using trace metal-substituted goethite have observed that roughly 5−30% of preincorporated trace metals are released when the mineral is exposed to aqueous Fe^{2+}.[1,3−5] These observations have been difficult to reconcile with the majority of isotopic tracer studies[5,17,18,22,27,32] that estimate 60−100% isotopic mixing. In contrast, the reported release of trace elements (5−30%) is somewhat consistent with the estimates of the recrystallization extent (14−20%) based on a gradual and partial back-reaction model over similar experimental time scales.[19,25] To the best of our knowledge, there have been no attempts to compare the isotope-derived and trace element-derived recrystallization within the same study, precluding a direct comparison of these two approaches.

To address this knowledge gap, this study aimed to probe the mineral dynamics of Fe^{2+}-catalyzed goethite recrystallization using a combined experimental and modeling approach. The specific case of U-incorporated goethite was tackled, due to the particular interest in U as a redox-sensitive trace metal of relevance for modern and paleo environments, and thus its potential to probe redox coupling during Fe^{2+}-catalyzed recrystallization. U was incorporated into the goethite structure during its synthesis. A ^{57}Fe-enriched Fe^{2+} tracer was employed to investigate the atom exchange between aqueous $^{57}Fe^{2+}$ and Fe(III) in goethite. By combining solid-phase characterization, data on U release during Fe^{2+}-activated iron (oxyhydr)oxide recrystallization, Fe isotope dynamics, and process modeling, we quantitatively evaluated the fraction of goethite recrystallization as a result of partial and gradual back reaction. This work enhances our understanding of mineral dynamics via the recrystallization of Fe^{2+}-catalyzed iron (oxyhydr)oxide.

MATERIALS AND METHODS

Synthesis of U-Containing Goethite. All reagents and chemicals utilized in the study were of ACS grade, except for HCl, which was of Optima grade and reserved for samples designated for isotope analysis. All experiments were performed within an anoxic chamber (MBraun, ~100% N_2, O_2 level <0.1 ppm), unless otherwise indicated. Solutions were prepared with Milli-Q water (18.2 MΩ·cm) and were thoroughly degassed with pure N_2 prior to use. All glassware and stoppers were cleaned using analytical grade HCl, followed by Optima grade HCl and Milli-Q water before use.

Two-line ferrihydrite of natural Fe isotope abundance was synthesized as described in Supporting Information Text S1. Its mineralogy and morphology were examined with X-ray diffraction (XRD, Figure S1A) and transmission electron microscopy (TEM, Figure S2A). U-incorporated goethite (abbreviated U-goe, containing 22.22 mM as Fe, 108 μM as U, with a U/Fe molar ratio of ~1:206 and a U content of ~20.24 mg U per g solid) was prepared through Fe^{2+}-induced ferrihydrite transformation in the presence of U(VI).[7] This synthesis pathway was chosen because it allows for more effective and more homogeneous U incorporation and reflects near-surface environmental conditions, whereas hydrothermal

https://doi.org/10.1021/acs.est.5c11748
Environ. Sci. Technol. XXXX, XXX, XXX−XXX

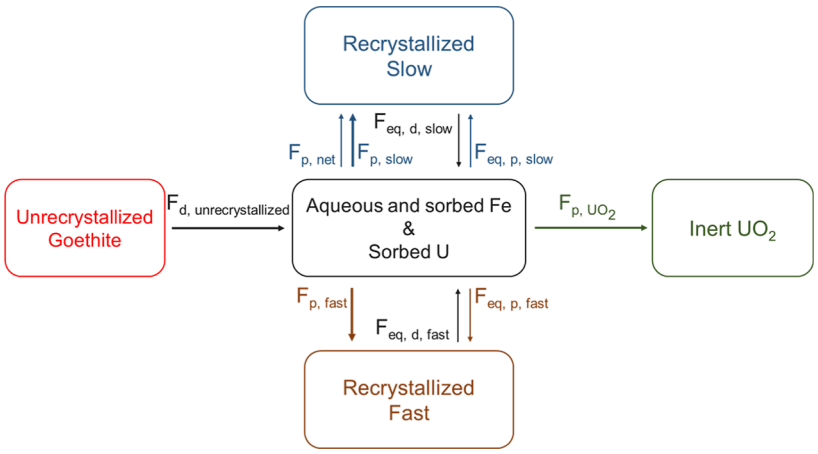

Figure 2. Schematic representation of dissolution and precipitation processes during Fe^{2+}-catalyzed recrystallization of U-goethite. The model was constructed based on the following conceptual framework: (i) unrecrystallized goethite dissolves into the aqueous phase, (ii) Fe^{2+} precipitates from the aqueous phase as recrystallized goethite, (iii) the recrystallized solid redissolves and (iv) reprecipitates. Processes (iii) and (iv) are referred to as the back-reaction over two time scales: fast and slow. Each box represents an iron reservoir. The arrows between boxes represent the dissolution and precipitation fluxes during recrystallization, assumed to proceed via the 0.5 M HCl extraction pool. In addition, we assume that part of the uranium moves from the 0.5 M HCl extraction into a UO_2 pool that is inert.

synthesis requires elevated temperature and pressure, and yields a U-goethite that is relatively inert to Fe^{2+}-catalyzed recrystallization.[8,33−35] More details on the preparation of U-incorporated goethite are included in Supporting Information Text S2, Figures S3 and S4. XRD patterns and TEM images of U-goethite prior to and post acid extraction are illustrated in Figures S1B,S2B,C.

Atom Exchange. Atom exchange experiments (Figure 1) were conducted to investigate the geochemical persistence of structurally incorporated U in goethite using a combined isotope tracer[17] and incorporated trace element release[1] approach. A ^{57}Fe-enriched aqueous Fe^{2+} stock ($\delta^{57/56}Fe$ = 133.43%) was prepared by mixing $^{57}Fe^{2+}Cl_2$ (Eurisotop, 95.08% ^{57}Fe) with a $Fe^{2+}Cl_2$ stock of natural isotope abundance. Two conditions were selected (Figure 1): (1) Aging in PIPES as a control (abbreviated U-goe-ctl) in which U-incorporated goethite (U-goe, containing 22.22 mM as Fe, 108 μM as U) was aged in 25 mM PIPES buffer (pH 7.5) for 30 d; (2) Amendment with $^{57}Fe^{2+}$ (abbreviated U-goe-Fe) as a treatment in which the same U-goe suspension was mixed with 1 mM freshly prepared ^{57}Fe-enriched isotope tracer in 25 mM PIPES buffer (pH 7.5). The pH was selected to ensure consistency with typical Fe^{2+}-catalyzed goethite recrystallization studies.[17−20,25] Figure 1 offers a schematic of the experimental manipulations including the sample separation procedures. All reactions were performed in duplicate within an anoxic chamber in the dark. Measured pH values changed by less than 0.1 during the reaction time frame.

At preselected time points, an aliquot of the suspension was centrifuged at 3000g for 5 min. The supernatant was filtered through 0.22 μm PTFE filters and the filtrate was referred to with a "-aq" suffix (Figure 1). The pellet was digested in 6 M HCl and referred to with a "-s" suffix (Figure 1). Both filtrate and pellet were analyzed for Fe and U concentrations.

For atom exchange reactions (those in which $^{57}Fe^{2+}$ was amended), it was important to distinguish the Fe isotope signal coming from bulk goethite from that of amended Fe^{2+}. Handler et al. (2014)[18] showed that 0.4 M HCl selectively extracts sorbed/aqueous species from goethite while leaving the crystalline lattice intact. Consistently, earlier studies by Jang et al. (2008),[36] Sidhu et al. (1981)[37] and Zachara et al. (2001)[38] demonstrated that 0.5 M HCl effectively differentiates highly crystalline iron (oxyhydr)oxide (e.g., goethite) from a mixture of Fe^{2+}, U(VI), ferrihydrite and U(IV) minerals. Therefore, 0.5 M HCl was employed to ensure quantitative removal of sorbed and aqueous species. The goethite suspension (1 mL) was equilibrated with 1 mL of 1 M HCl solution (Optima grade, final concentration 0.5 M) for 30 min, the mixture was centrifuged at 3000g for 5 min, so as to separate the remaining pellet (e.g., U-goe-Fe-HCl-s, goethite) from the acid extractable fraction (e.g., U-goe-Fe-HCl-aq, aqueous and sorbed Fe, sorbed U, and UO_2) (Figure 1). The extracted aqueous phase was filtered through a PTFE filter (0.22 μm). Aliquots of the filtrate and parts of the pellet (the latter after 6 M HCl digestion) were analyzed for U and Fe concentrations as well as Fe isotope composition. The acid extractable filtrate was also analyzed for Fe^{2+} content, while the postextraction pellet solid was characterized by XRD, TEM, ^{57}Fe Mössbauer spectroscopy and X-ray absorption spectroscopy (XAS).

Aqueous Phase and Isotope Analysis. Aqueous samples, including 0.5 M HCl extractable aqueous phase and 6 M HCl digested solids, were measured for Fe and U concentrations with inductively coupled plasma mass spectrometry (ICP−MS). The aqueous Fe^{2+} concentration in the postextraction filtrate was measured following the Ferrozine method.[39,40] Fe isotope analyses were conducted at the Leibniz University Hannover in Germany employing a Thermo Scientific-Neptune multicollector inductively coupled plasma source mass spectrometer (MC-ICP-MS).[41] More details regarding Fe isotope measurements are provided in Supporting Informtion Text S3.

Solid Phase Characterization. The mineralogy and morphology of U-incorporated goethite (post 0.5 M HCl extraction, unless otherwise stated) were characterized via diffractometry, spectroscopy and electron microscopy methods, including XRD, TEM and ^{57}Fe Mössbauer spectroscopy (Supporting Information Text S4). The valence state of U was determined by M_4-edge high-energy-resolution fluorescence detection X-ray absorption near-edge structure spectroscopy

https://doi.org/10.1021/acs.est.5c11748
Environ. Sci. Technol. XXXX, XXX, XXX−XXX

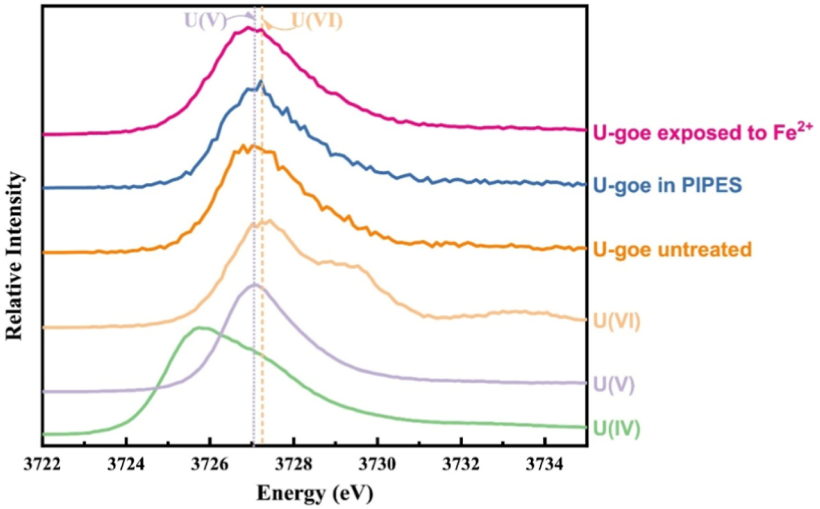

Figure 3. U M_4-edge HERFD-XANES spectra of U-incorporated goethite prior to and post atom exchange. A set of standards including U(IV) as UO_2, U(V) as KUO_3, and U(VI) as UO_2^{2+} adsorbed on pure goethite were included for comparison. Dotted and dashed lines indicate the white line energy positions for U(V) and U(VI) valence states, respectively. All goethite samples were 0.5 M HCl extracted prior to analysis. "U-goe untreated" refers to the original U-incorporated goethite sample, while "U-goe in PIPES" denotes the U-incorporated goethite aged in 25 mM PIPES buffer (pH 7.5) for 30 days.

(M_4-edge HERFD XANES).[41] More details are described in Supporting Information Text S5.

Modeling. To quantify the fraction of goethite recrystallized, isotopic dynamics of Fe and bulk dynamics of U were cosimulated during Fe^{2+}-catalyzed recrystallization of U-goethite. A box model (Figure 2) that included partial and gradual back-reaction was utilized to constrain the rate of recrystallization from isotopic data collected in laboratory experiments, similar to the framework in Joshi et al. (2022),[25] where we simulated the isotopic changes in pure goethite recrystallization.

In brief, the model simulated the temporal evolution of Fe and U masses as well as the Fe isotopic composition across different reservoirs (Figure 2). Following Joshi et al. (2022),[25] the reservoirs individually represent (a) the unrecrystallized U-goethite, (b) the slowly back-reacting recrystallized U-goethite, (c) the fast back-reacting recrystallized U-goethite and, in addition, (d) a reservoir consisting of the aqueous and sorbed species. This reservoir was included as the isotopic composition of Fe and the mass of U was measured not in the aqueous phase but in an extraction using 0.5 M HCl. This treatment selectively dissolves aqueous and sorbed Fe, sorbed U (no aqueous U was detected, Figure S5A and Table S1), and UO_2, while leaving the bulk U-goethite intact. We assume that all dissolution and reprecipitation fluxes go through the reservoir that contains aqueous and sorbed Fe, and sorbed U (referred to as the "aq + sorbed" reservoir, Figure 2). The 0.5 M HCl extracted fraction corresponds to the "aq + sorbed" reservoir in the box model, analogous to the aqueous reservoir in Joshi et al. (2022).[25] Furthermore, we included a precipitated UO_2 reservoir that was assumed to be derived from the "aq + sorbed" reservoir.[42] The rest of the goethite (digested by 6 M HCl) is therefore composed of recrystallized and unrecrystallized goethite.

The mass of Fe or U in each reservoir was simulated to evolve over time according to fluxes that add or remove mass

$$\frac{dN_i}{dt} = \sum F_{in} - \sum F_{out} \quad (1)$$

where N_i is the mass of Fe or U in reservoir i (moles), F_{in} is the flux into the reservoir (mol day^{-1}), F_{out} is the flux out of the reservoir (mol day^{-1}), and Σ represents the sum over all input or output fluxes. The fluxes were governed by the size of the reservoirs and the rate of recrystallization, which had the following form

$$R_i = a_i \times \exp\left(\frac{-t}{b_i}\right) \quad (2)$$

where a_i is the rate constant (% day^{-1}) and b_i is the time scale over which the flux approaches zero (days). An exponentially decaying rate was chosen because (a) our previous work[19] showed that the recrystallization rate decreases over time, and (b) this formulation provides sufficient generality without introducing an unnecessary number of parameters. The recrystallized reservoirs back-reacted with the "aqueous + sorbed" reservoir over a turnover time τ_i (days). The evolution of U masses within the different pools was simulated via coupling to the fluxes of Fe: (a) in the case of dissolution, the flux was proportional to the solid molar ratio U:Fe, and (b) in the case of precipitation, the flux was proportional to the aqueous molar ratio U:Fe as well as a distribution coefficient $D_{k,U}$ The isotopic compositions of the reservoirs changed according to Fantle and Tipper (2014).[43]

$$\frac{dr_i}{dt} = \sum \frac{F_{j-i}}{N_i} \times (\alpha_{F_{j-i}} \times r_j - r_i) \quad (3)$$

Details of model construction are described in Supporting Information Text S6. After setting up the model equations, the rate parameters (a_i, b_i, τ_i and $D_{k,U}$, where i denotes the fast or slow back-reacting recrystallization) were optimized by minimizing the differences between the simulated and measured values of U masses and ^{57}Fe isotopic ratios using the genetic optimization algorithm.[44,45]

RESULTS AND DISCUSSION

Characterization of U-Incorporated Goethite. The incorporation of uranium into goethite was confirmed through

https://doi.org/10.1021/acs.est.5c11748
Environ. Sci. Technol. XXXX, XXX, XXX−XXX

Table 1. LCF Analysis of U M_4-Edge HERFD-XANES Spectra of 0.5 M HCl Extracted U-Incorporated Goethite Prior to and Post Isotope Exchange

sample type	U (VI)		U (V)		U (IV)		R factor	reduced $\chi 2$
	percentage	STD	percentage	STD	percentage	STD		
untreated	8.57	2.75	91.43	4.51	-	-	0.02102	0.00130
aged in PIPES	2.73	3.52	97.27	2.41	-	-	0.01937	0.00100
Fe^{2+} amendment	8.62	5.20	91.38	4.13	-	-	0.04508	0.00293

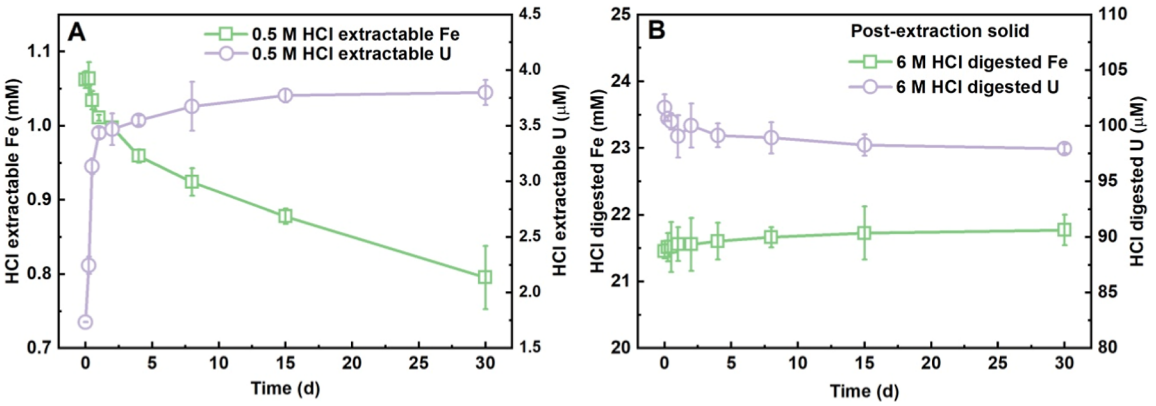

Figure 4. Time-course variations in the U-goe-Fe^{2+} system. (A) 0.5 M HCl extractable Fe and U and (B) Fe and U contents in the remaining solid digested with 6 M HCl.

a combination of wet chemical, mineralogical, and spectroscopic techniques. The homogeneity of the distribution of U atoms within the goethite structure was estimated via time-dependent acid digestion of the suspension with 6 M HCl. The Fe and U concentrations eventually reached a plateau after 4 h, and 53.51 μM out of 100.73 μM U(VI) (initial U concentration mixed with ferrihydrite) was found to be incorporated into the goethite structure (Figure S6A). The simultaneous increase of digested Fe and U concentrations, with a linear relationship between the two (Figure S6B), suggests a homogeneous distribution of U atoms within the goethite structure, with an Fe/U proportion of 11.45 mM Fe to 53.51 μM U.

The mineralogical analysis by XRD revealed goethite as the only mineral phase (Figure S1B), while the TEM images showed the typical acicular goethite morphology, with nanorods reaching ~500 nm in length and ~10 nm in width, corresponding to a BET surface area of 54.3 m^2 g^{-1} (Figure S2C). These values fall within the range commonly reported for goethite used in Fe^{2+}-catalyzed recrystallization studies.[33−35] ^{57}Fe Mössbauer spectra confirmed these observations by exhibiting two sextets, with center shift values of 0.45 to 0.48 mm/s, quadrupole shifts (ε) of −0.15 to −0.13 mm/s, and hyperfine field strength values of 47.3 to 49.4 T, both corresponding to goethite but with varying crystallinity (Figure S7A and Table S2), likely arising from differences in particle size, lattice defects, and U incorporation during Fe^{2+}-catalyzed transformation. Deconvoluting the contributions of these processes is beyond the scope of this study as it would involve extensive spectromicroscopic investigations. The U valence state in U-goethite determined by M_4-edge HERFD-XANES revealed a majority (~91%) of U(V) (Figure 3 and Table 1) post 0.5 M HCl extraction. Although the characteristic peaks of U(VI) and U(V) are only subtly distinguishable by visual inspection (Figure 3), LCF analysis provides more direct and quantitative evidence for U valence states (Table 1), confirming that U(V) is the predominant species in U-goethite. Moreover, the postedge peak at 3729.5 eV. characteristic for uranyl structure, was missing for U-goethite when compared to uranyl(VI) adsorbed onto goethite, which is consistent with previous studies on the formation of uranate(V) as the dominant chemical state,[7,8] and suggested the successful removal of most surface U(VI) and U(IV) by 0.5 M HCl.

Chemical and Structural Stability of U-Incorporated Goethite under Anoxic Condition. To test the intrinsic stability of U-goethite, it was placed in an anoxic PIPES-buffered solution as a control (achieving ~21.4 mM as Fe, ~101 μM as U in the solid). It remained stable throughout the experimental period (30 d). No dissolved Fe or U were detected in the aqueous phase, while only ~20 μM Fe and ~0.1 μM U were released during a 30 min extraction with 0.5 M HCl solution (Table S1), accounting for ~0.1% of U-goethite dissolution. This observation demonstrated that 0.5 M HCl effectively extracts sorbed/aqueous species while causing minimal U-goethite dissolution. No obvious changes in morphology (Figure S2D), mineralogy (Figures S7B, S8 and Table S2) or U valence states (Figure 3 and Table 1) were observed after the 30-d incubation for the control system.

Fe^{2+}-Catalyzed Goethite Recrystallization and U Mobilization. Rapid adsorption of aqueous Fe was observed when introducing 1.06 mM $^{57}Fe^{2+}$ to the U-goethite suspension, with the immediate aqueous Fe being measured as 0.56 mM, which then gradually decreased to 0.38 mM after 30 d (Figure S5A). Correspondingly, the concentration of solid-associated Fe increased from 21.82 to 22.03 mM (Figure S5B). Meanwhile, aqueous U was not detected, and the concentration of solid-associated U remained relatively stable at ~100 μM throughout the experiment (Figure S5B). Unlike the control system (aging in PIPES) for which only ~0.1 μM U was released through 0.5 M HCl extraction (Table S1), the addition of 1.06 mM Fe^{2+} resulted in 3.9 μM of 0.5 M HCl-extractable U after 15 d (Figure 4A), including trace amount of UO_2 precipitates (Figure S2E), corresponding to a slight

https://doi.org/10.1021/acs.est.5c11748
Environ. Sci. Technol. XXXX, XXX, XXX−XXX

decrease in goethite-associated U (Figure 4B). It is worth noting that extractable Fe (Figure 4A) and Fe^{2+} (Figure S9) showed a decreasing trend with time, while the concentration of solid-associated Fe (Figure 4B) and Fe^{2+} (Figure S9) showed a slight increase. This suggests that a proportion of amended Fe^{2+} (~25%) enters the goethite structure, which may form Fe(II)-containing solid-phase or exist as spinel-like phases containing Fe(II) within the iron (oxyhydr)oxide lattice that was not extracted by 0.5 M HCl. The contribution of U(VI) reduction to Fe^{2+} oxidation is negligible: only 3.9 μM of U was mobilized (Figure 4A), and structurally incorporated U was confirmed to remain predominantly as U(V) before and after reaction (Figure 3), ruling out significant U(VI)−Fe(II) redox coupling. Similar Fe^{2+} incorporation has been previously observed for goethite[36] and hematite,[46,47] possibly through interfacial electron transfer followed by structural rearrangement, thereby extending the relevance of our findings to a broad range of natural systems. However, due to the low amount of newly entered Fe species (~0.26 mM) relative to the Fe in the goethite (~22 mM), the newly formed Fe(II)-containing phase was not detected by XRD, TEM or ^{57}Fe Mössbauer spectroscopy, where only the goethite phase or needle-shaped goethite particles were observed (Figures S2F, S7C, S8 and Table S2).

The Fe isotopic measurement confirms the atom exchange process after introduction of Fe^{2+} to U-goethite suspension (Figure 5). The isotopic composition of the acid-extracted Fe

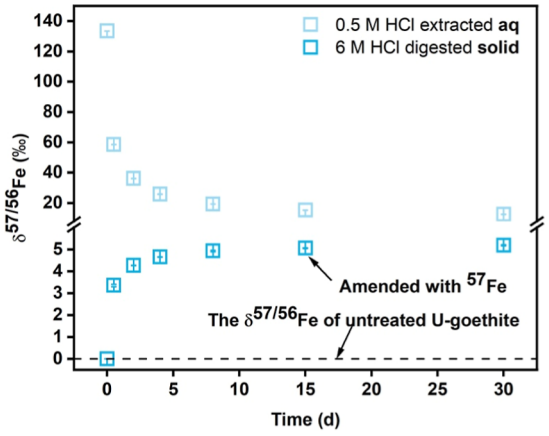

Figure 5. Fe isotope signatures in 0.5 M HCl extracted aqueous phase and in the remaining solid phase digested with 6 M HCl for U-goethite amended with $^{57}Fe^{2+}$ system, corresponding to the 0.5 M HCl extractable Fe and 6 M HCl digested Fe phases that were measured in Figure 4. The dashed line represents the $\delta^{57/56}$Fe value of untreated U-goethite.

gradually decreases from an initial $\delta^{57/56}$Fe of 133.43‰ to 12.57‰, while that in the solid phase increases from 0.01‰ to 5.19‰. Such a trend has been reported in several previous studies that revealed the iron conveyor belt behavior during the mixing of Fe^{2+} with goethite,[17−20,25] magnetite,[22,48] and hematite,[49,50] where the heavier Fe atoms in the solution exchange with the lighter Fe atoms in mineral phase (natural abundance). Even if UO_2 formed as a result of U(VI) reduction (Figure S2E), the redox coupling between sorbed Fe^{2+} and U(VI) (3.9 μM, Figure 4A) accounts for only a minor fraction of the total Fe flux in goethite (~22 mM, Figure 4B). Therefore, its impact on Fe isotopic fractionation is negligible.

The role of particle size and specific surface area in Fe^{2+}-catalyzed recrystallization was also considered. U-goethite in this study (nanorods ~500 × 10 nm, BET 54.3 m^2 g^{-1}) is comparable to sizes reported in previous isotope tracer studies, where extensive Fe atom exchange was observed with only minor dependence on primary particle size at the tested pH value (7.5).[18,51] Thus, under our experimental conditions, particle size is unlikely to have strongly influenced the extent of U-goethite recrystallization.

Though Fe atomic exchange occurred, and U was partially released, the white line position of U-goethite-Fe^{2+} M_4 HERFD-XANES spectra after 30 d reaction did not show a significant shift as compared to the U-goethite or U-goethite-PIPES (Figure 3). LCF analysis indicated that the incorporated U in goethite still mainly existed as U(V) form (>91%, Table 1), suggesting the stability of U valence state under reducing conditions, and is consistent with previous observations that structural U(V) can stably persist in reducing environments.[8]

Mineral Dynamics of Fe^{2+}-Catalyzed Iron (Oxyhydr)-Oxide Recrystallization. Here, we used a ^{57}Fe-enriched isotopic tracer to probe the mineral dynamics of Fe^{2+}-catalyzed recrystallization of U-goethite. At the end of 30 days, the isotopic composition ($\delta^{57/56}$Fe) of both the acid extracted aqueous phase (12.57‰) and the remaining goethite solid (5.19‰) had shifted toward the calculated mass balance-weighted isotopic composition (5.93‰, Figure 5), indicating progressive mixing of isotopes between the two pools.[17] Similar isotopic trends have been observed, confirming Fe atom exchange between aqueous Fe^{2+} and goethite during recrystallization over time.[17−19,25,27,31] Yet, previous studies did not provide quantitative insights into how homogeneous goethite recrystallization occurred.

To address this question, we re-examined the methodology used to calculate the recrystallized fraction of Fe in goethite. Temporal changes in the isotopic composition of the aqueous and goethite Fe phases can, in principle, be used to determine the fraction of goethite recrystallized. However, such a calculation relies on a critical assumption regarding the degree of back-reaction between recrystallized goethite and Fe^{2+} (Figure 2). This assumption relates to the spatial distribution of the isotopic tracer within the recrystallized fraction, ultimately affecting the extent of recrystallization calculated from bulk isotopic data.[19,26]

If the back-reaction between recrystallized goethite and Fe^{2+} were instantaneous and complete (fast back-reaction only), i.e., if every Fe atom in the recrystallized solid back-reacted instantaneously with aqueous Fe^{2+}, the iron (oxyhydr)oxide would be isotopically homogeneous and in isotopic equilibrium with the aqueous Fe^{2+} (Figure 2).[17,18,27] Using a model that included only a fast back-reaction, the majority of previous studies have inferred extensive recrystallization of goethite (60−100%) over the time scale of weeks under similar experimental conditions (pH 7.5).[17,18,27] Consistent with these observations, we estimated 88% goethite recrystallization based on fast back-reaction only (Figure 5, calculation of percent recrystallization as described in Handler et al. (2014)[18]), which contrasts sharply with the measured release of U from substituted goethite (Figure 4A, 3.9 μM out of 100 μM, 3.9%). This discrepancy may arise from the high solid:aqueous Fe molar ratio (22.22:1) used in our experiment, comparable to that (20.2−22:1) in typical Fe^{2+}-catalyzed recrystallization studies.[17,18,27] In such scenario, the solid would have a high isotopic leverage in the system. Small changes in the solid

https://doi.org/10.1021/acs.est.5c11748
Environ. Sci. Technol. XXXX, XXX, XXX−XXX

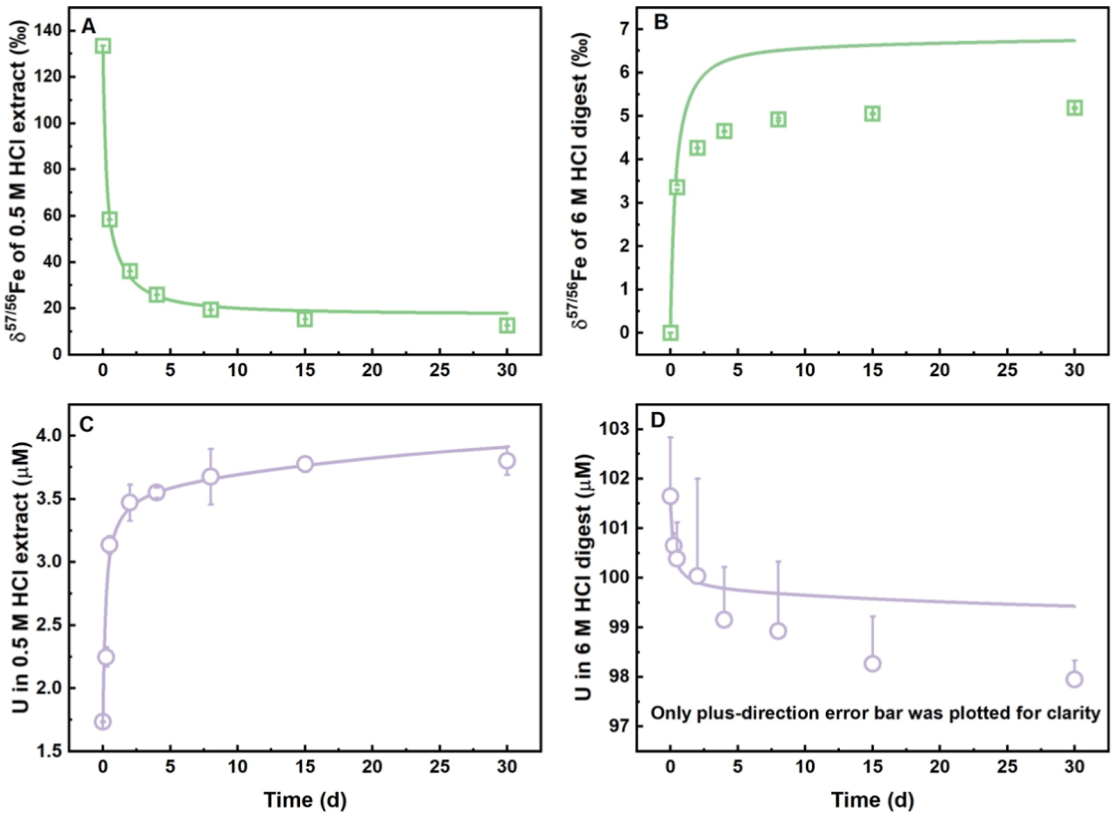

Figure 6. Measured (markers) and simulated (lines) values of (A) $\delta^{57/56}$Fe in 0.5 M HCl extracted and (B) 6 M HCl digested reservoirs, as well as (C) U concentration in 0.5 M HCl extracted and (D) 6 M HCl digested reservoirs.

isotopic composition result in large variations in the isotopic composition of the aqueous phase. In other words, large changes in the isotopic composition of the aqueous Fe cannot be readily interpreted as near-complete recrystallization of the solid. Therefore, the previously reported recrystallization extents of goethite (60−100%), based on the large variations in aqueous Fe isotopic compositions as a guideline, are most likely overestimates.

Furthermore, this discrepancy suggests the limitation of the fast back-reaction-only model in describing isotopic dynamics during goethite recrystallization, given the homogeneous distribution of U in U-substituted goethite (Figure S6B). Similar disparities have been documented among past isotopic tracer studies and trace element cycling investigations. Studies using trace metal-substituted goethite have reported roughly 5−30% of preincorporated trace metals release upon exposure to aqueous Fe^{2+},[1,3−5] reflecting differences in the identity of the trace elements and the host minerals. This range is consistent with our observed U release (Figure 4A, 3.9%), but well below the inferred fraction of recrystallization (~88%, Figure 5) based on the fast back-reaction-only model. Till now, consideration of different back-reaction scenarios has been limited by the availability of data sets consisting solely of Fe isotope data. By simultaneously considering the estimate of Fe isotope-derived recrystallization and the release of structurally incorporated trace elements within the same experiment, we aim to improve the isotope-derived model.

Therefore, we constructed a box model based on partial and gradual back-reaction (Figure 2) to simulate both the Fe isotopic dynamics and the U bulk dynamics, based on a previously constructed framework.[25] The Fe and U fluxes were coupled with a distribution coefficient ($D_{k,U}$, Supporting Information Text S6). The partial and gradual back-reaction model implies that the recrystallized solid back-reacts over a distribution of time scales rather than instantaneously (the latter corresponds to the fast back-reaction only). To simplify this distribution and to compare with the previously adopted fast back-reaction only model, we assumed that back-reaction occurs over two time scales, i.e., fast back-reaction and slow back-reaction. The model developed in Figure 2 describes the Fe and U fluxes with the following best fit parameters: a_{slow} = 1.04 ± 0.10% day^{-1}, b_{slow} = 11.49 ± 0.45 days, τ_{slow} = 5.93 × 10^2 ± 7.70 × 10^1 days, a_{fast} = 1.00 × 10^1 ± 0.03 × 10^1% day^{-1}, b_{fast} = 2.67 ± 0.02 days, τ_{fast} = 0.27 ± 0.03 days, $D_{k,U}$ = 1.32 ± 0.01, a_{UO_2} = 0.13 × 10^{-1} ± 0.06 × 10^{-2} day^{-1} (Supporting Information Text S6). Parameter optimization was performed using a genetic algorithm[44,45] constrained by the measured U masses and ^{57}Fe isotopic ratios, with a minimized sum of squared errors (SSE) of 4.88 × 10^{-4}. The rate parameters here are mostly comparable to those reported for pure goethite,[25] except for a_{fast}, i.e., the rate constant of formation of the fast back-reacting fraction, which was substantially higher in our experiment (1.00 × 10^1 ± 0.03 × 10^1% day^{-1}) than in previous reports (1.75 ± 0.01% day^{-1}~1.99 ± 0.03% day^{-1}).[25] The higher a_{fast} obtained in this study led to a substantially higher initial recrystallization rate of 22.34 μmol m^{-2} d^{-1} (Figure S10), compared to our previous reports (2.65 to 4.67 μmol m^{-2} d^{-1}).[25] The recrystallization rate gradually decreased to 1.05 × 10^{-1} μmol m^{-2} d^{-1} after 30 days (Figure S10), falling within the range of our earlier results (4.72 × 10^{-3} to 1.78 × 10^{-1} μmol m^{-2} d^{-1}).[25]

With these estimated parameters, the partial and gradual model matches the ^{57}Fe and U mass data in the 0.5 M HCl

https://doi.org/10.1021/acs.est.5c11748
Environ. Sci. Technol. XXXX, XXX, XXX−XXX

extraction reservoir well (Figure 6A,C). The model also matches the overall trends of the ^{57}Fe and U mass in the 6 M HCl extraction reservoir (Figure 6B,D), though not perfectly, possibly due to the partial reincorporation of released U into goethite during recrystallization, which leads to an underestimation of the true extent of U mobilization. Moreover, the formation of UO_2 via the reductive precipitation of released U (Figure S2E), which cannot be reincorporated into the mineral structure during the back-reaction of recrystallized goethite, weakens the link between goethite recrystallization and U cycling, making U release an inconsistent reflection of the extent of iron (oxyhydr)oxides recrystallization. Employing a conservative tracer may provide a more robust approach in future studies. Based on this partial and gradual model, the overall extent of recrystallization was estimated to be 32.8%, with a slow back-reacting fraction of 9.7% and a fast back-reacting fraction of 23.1% (Spporting Information Text S6). The estimates of recrystallization extent are slightly different from past studies (e.g., overall recrystallization faction of 14−20%, with >80% being slow back-reacting fraction),[25] likely due to the presence of U within the original goethite (e.g., U-goethite) rather than pure goethite. The higher fast back-reacting fraction suggests that structural incorporation of U enhances the susceptibility of goethite to rapid back-reaction. This may be associated with the broader crystallinity distribution in U-goethite than in pure goethite, as evidenced by the presence of two goethite sextets in the ^{57}Fe Mössbauer spectra (Figure S7 and Table S2). Notably, the coexistence of two crystallinities does not contradict the homogeneous distribution of U in goethite, as indicated by synchronous dissolution behavior of Fe and U (Figure S6); rather, it reflects local structural variations inherent to the synthesis of nanoparticulate goethite.

While this study focuses on uranium, the partial and gradual back-reaction model may also be conceptually extended to other trace elements incorporated in goethite. However, some redox-active trace elements may encounter a similar limitation as U. Their reduced products (e.g., Se^0) may not be readily reincorporated into the goethite structure during recrystallization.

Environmental Implications. Iron (oxyhydr)oxides have been proposed as geological proxies for the reconstruction of paleoenvironmental conditions, as their isotopic and elemental compositions in the geological rock record are functionally linked to the geological events throughout Earth's history.[52−54] The dynamics of Fe^{2+}-catalyzed recrystallization observed in experimental systems can overprint the original iron (oxyhydr)oxide isotopic and elemental compositions and therefore needs to be accounted for in any proxy-based interpretation. Previous studies have reported extensive to nearly complete recrystallization of goethite over time scales of weeks,[17,18,22] suggesting a thorough reset of isotopic and elemental compositions in iron (oxyhydr)oxides. If this were the case, the isotopic compositions of iron (oxyhydr)oxides in natural settings would be expected to reset to natural abundance periodically. However, a wide range of isotopic compositions has been observed in iron (oxyhydr)oxides,[54] and attributed to environmental conditions during precipitation and/or diagenesis, supporting our assertion that Fe^{2+}-catalyzed recrystallization has a negligible effect on the isotopic composition of iron (oxyhydr)oxides in natural environments.[25] This is likely due to the high solid:aqueous Fe molar ratios commonly found in natural systems, where the limited isotopic leverage of the aqueous phase is insufficient to significantly alter the solid phase.

Our findings provide important implications not only for paleoenvironmental reconstructions but also for modern trace elements dynamics. Fe^{2+}-catalyzed iron (oxyhydr)oxide recrystallization, coupled to the release and redistribution of structurally incorporated trace elements, underscores the dynamic nature of iron (oxyhydr)oxides in subsurface environments. The partial release of U during recrystallization (3.9%) highlights the potential for iron oxides to act as both sinks and sources for trace elements. This dual role could influence the fate and transport of trace elements in nature, particularly under fluctuating redox conditions. The partial and gradual back-reaction model established here demonstrates that trace-element release from recrystallizing iron oxides occurs progressively rather than completely. This mechanistic understanding is highly relevant for predicting uranium mobility in contemporary settings such as groundwater, mining residues, and contaminated soils, where Fe^{2+}-goethite interactions often govern the fate of trace elements. By capturing the incremental release and partial reincorporation of trace elements, our model improves the accuracy of contaminant transport predictions over long time scales, informing risk assessment and remediation strategies.

The modeling results of partial and gradual back-reactions further emphasizes that traditional assumptions of rapid and complete isotopic equilibration may lead to overestimated extents of recrystallization and contaminant mobilization, especially under high solid to aqueous ratios. This insight is critical for remediation efforts, such as the use of reactive iron barriers, which rely on the stability and reactivity of iron (oxyhydr)oxides to immobilize contaminants. Understanding the kinetics of iron (oxyhydr)oxide recrystallization and its influence on trace element release can guide more effective designs and operational strategies for long-term contaminant sequestration, particularly for heavy metals and radionuclides. Thus, beyond serving as a paleo-proxy framework, the model directly contributes to evaluating environmental stability and guiding management of modern uranium-impacted sites.

Overall, our findings emphasize the complex and gradual nature of Fe^{2+}-catalyzed iron (oxyhydr)oxide recrystallization, with important consequences for the mobility and long-term fate of contaminants in the environment. Moreover, our results underscore the need for more nuanced models of trace metal behavior that account for varied time scales of mineral transformations, which are essential for accurate environmental risk assessments and the development of sustainable mitigation approaches.

■ ASSOCIATED CONTENT

Data Availability Statement

All relevant data are available from the authors or within the Supporting Information files. Raw data, including isotope information for each measurement, are available from a data repository as https://doi.org/10.5281/zenodo.17451826.

Supporting Information

The Supporting Information is available free of charge at https://pubs.acs.org/doi/10.1021/acs.est.5c11748.

Synthesis and characterization of 2-line ferrihydrite and U-incorporated goethite; experimental details for Fe isotope analysis, ^{57}Fe Mössbauer spectroscopy and M_4-edge HERFD XANES analysis; construction details for

https://doi.org/10.1021/acs.est.5c11748
Environ. Sci. Technol. XXXX, XXX, XXX−XXX

the gradual and partial box model; additional results for time-course variations of aqueous and acid-extracted Fe and U, solid-phase characterization and U-goethite recrystallization kinetics (PDF)

AUTHOR INFORMATION

Corresponding Authors

Zezhen Pan − *Environmental Microbiology Laboratory, Ecole Polytechnique Fédérale de Lausanne, Lausanne 1015, Switzerland; Department of Environmental Science and Engineering and National Observations and Research Station for Wetland Ecosystems of the Yangtze Estuary, Institute of Eco-Chongming, Fudan University, Shanghai 200433, China;* orcid.org/0000-0003-1712-3149; Email: zezhenpan@fudan.edu.cn

Hailiang Dong − *Center for Geomicrobiology and Biogeochemistry Research, State Key Laboratory of Biology and Environmental Geology, China University of Geosciences, Beijing 100083, China;* orcid.org/0000-0002-7468-1350; Email: dongh@cugb.edu.cn

Rizlan Bernier-Latmani − *Environmental Microbiology Laboratory, Ecole Polytechnique Fédérale de Lausanne, Lausanne 1015, Switzerland;* orcid.org/0000-0001-6547-722X; Email: rizlan.bernier-latmani@epfl.ch

Authors

Qingyin Xia − *Center for Geomicrobiology and Biogeochemistry Research, State Key Laboratory of Biology and Environmental Geology, China University of Geosciences, Beijing 100083, China; Environmental Microbiology Laboratory, Ecole Polytechnique Fédérale de Lausanne, Lausanne 1015, Switzerland;* orcid.org/0000-0001-7263-8212

Prachi Joshi − *Geomicrobiology, Department of Geosciences, University of Tuebingen, Tuebingen 72076, Germany; Swiss Federal Institute for Forest, Snow and Landscape Research WSL, Birmensdorf CH-8903, Switzerland;* orcid.org/0000-0001-5954-0309

Marina Lazarov − *Institute of Earth System Sciences, Leibniz University Hannover, Hannover D-30167, Germany;* orcid.org/0000-0001-7522-1164

Barbora Bartova − *Environmental Microbiology Laboratory, Ecole Polytechnique Fédérale de Lausanne, Lausanne 1015, Switzerland*

Xiyang Xu − *Geomicrobiology, Department of Geosciences, University of Tuebingen, Tuebingen 72076, Germany*

Tim Prüssmann − *Institute for Nuclear Waste Disposal (INE), Karlsruhe Institute of Technology, Karlsruhe 76021, Germany;* orcid.org/0000-0002-7903-9199

Andreas Kappler − *Geomicrobiology, Department of Geosciences, University of Tuebingen, Tuebingen 72076, Germany;* orcid.org/0000-0002-3558-9500

Stefan Weyer − *Institute of Earth System Sciences, Leibniz University Hannover, Hannover D-30167, Germany;* orcid.org/0000-0001-7734-4571

Complete contact information is available at: https://pubs.acs.org/10.1021/acs.est.5c11748

Author Contributions

The manuscript was written through contributions from all authors. Z.P. and R.B.L. conceived of the research. Q.X. performed the experiments with support from M.L. and S.W. who conducted the Fe isotope measurement, B.B. who performed the STEM analysis, P.J., X.X and A.K. who conducted ^{57}Fe Mössbauer spectroscopy measurements, T.P. who assisted with the HERFD-XANES measurements and P.J. who constructed the box model. All authors gave their approval for the final version of the manuscript.

Notes

The authors declare no competing financial interest.

ACKNOWLEDGMENTS

Funding for this research was provided by the National Natural Science Foundation of China (42407333 and 42107228), Swiss National Science Foundation Grant (200021E-164209 and 200021-204922) and European Research Council Consolidator Grant 725675 (UNEARTH). The authors acknowledge the KIT light source for provision of beamtime at the ACT Beamline operated by the Institute for Nuclear Waste Disposal (INE) and thank the Institute for Beam Physics and Technology (IBPT) for the operation of the storage ring, the Karlsruhe Research Accelerator (KARA).

REFERENCES

(1) Frierdich, A. J.; Luo, Y.; Catalano, J. G. Trace element cycling through iron oxide minerals during redox-driven dynamic recrystallization. *Geology* **2011**, *39* (11), 1083−1086.

(2) Frierdich, A. J.; Scherer, M. M.; Bachman, J. E.; Engelhard, M. H.; Rapponotti, B. W.; Catalano, J. G. Inhibition of trace element release during Fe(II)-activated recrystallization of Al-, Cr-, and Sn-substituted goethite and hematite. *Environ. Sci. Technol.* **2012**, *46* (18), 10031−10039.

(3) Frierdich, A. J.; Catalano, J. G. Fe(II)-mediated reduction and repartitioning of structurally incorporated Cu, Co, and Mn in iron oxides. *Environ. Sci. Technol.* **2012**, *46* (20), 11070−11077.

(4) Frierdich, A. J.; Catalano, J. G. Controls on Fe(II)-activated trace element release from goethite and hematite. *Environ. Sci. Technol.* **2012**, *46* (3), 1519−1526.

(5) Latta, D. E.; Gorski, C. A.; Scherer, M. M. Influence of Fe^{2+}-catalysed iron oxide recrystallization on metal cycling. *Biochem. Soc. Trans.* **2012**, *40* (6), 1191−1197.

(6) Ilton, E. S.; Collins, R. N.; Ciobanu, C. L.; Cook, N. J.; Verdugo-Ihl, M.; Slattery, A. D.; Paterson, D. J.; Mergelsberg, S. T.; Bylaska, E. J.; Ehrig, K. Pentavalent Uranium Incorporated in the Structure of Proterozoic Hematite. *Environ. Sci. Technol.* **2022**, *56* (16), 11857−11864.

(7) Massey, M. S.; Lezama-Pacheco, J. S.; Jones, M. E.; Ilton, E. S.; Cerrato, J. M.; Bargar, J. R.; Fendorf, S. Competing retention pathways of uranium upon reaction with Fe(II). *Geochim. Cosmochim. Acta* **2014**, *142*, 166−185.

(8) Stagg, O.; Morris, K.; Lam, A.; Navrotsky, A.; Velázquez, J. M.; Schacherl, B.; Vitova, T.; Rothe, J. r.; Galanzew, J.; Neumann, A.; et al. Fe(II) induced reduction of incorporated U(VI) to U(V) in goethite. *Environ. Sci. Technol.* **2021**, *55* (24), 16445−16454.

(9) Marshall, T. A.; Morris, K.; Law, G. T.; Livens, F. R.; Mosselmans, J. F. W.; Bots, P.; Shaw, S. Incorporation of uranium into hematite during crystallization from ferrihydrite. *Environ. Sci. Technol.* **2014**, *48* (7), 3724−3731.

(10) Nico, P. S.; Stewart, B. D.; Fendorf, S. Incorporation of oxidized uranium into Fe (hydr)oxides during Fe(II) catalyzed remineralization. *Environ. Sci. Technol.* **2009**, *43* (19), 7391−7396.

(11) Xiao, W.; Jones, A. M.; Li, X.; Collins, R. N.; Waite, T. D. Effect of Shewanella oneidensis on the kinetics of Fe(II)-catalyzed transformation of ferrihydrite to crystalline iron oxides. *Environ. Sci. Technol.* **2018**, *52* (1), 114−123.

(12) Boland, D. D.; Collins, R. N.; Glover, C. J.; Payne, T. E.; Waite, T. D. Reduction of U(VI) by Fe(II) during the Fe(II)-accelerated

https://doi.org/10.1021/acs.est.5c11748
Environ. Sci. Technol. XXXX, XXX, XXX−XXX

transformation of ferrihydrite. *Environ. Sci. Technol.* **2014**, *48* (16), 9086−9093.
(13) Moyes, L. N.; Parkman, R. H.; Charnock, J. M.; Vaughan, D. J.; Livens, F. R.; Hughes, C. R.; Braithwaite, A. Uranium uptake from aqueous solution by interaction with goethite, lepidocrocite, muscovite, and mackinawite: An X-ray absorption spectroscopy study. *Environ. Sci. Technol.* **2000**, *34* (6), 1062−1068.
(14) Liu, Y.; Ding, Y.; Sheng, A.; Li, X.; Chen, J.; Arai, Y.; Liu, J. Fe(II)-catalyzed transformation of ferrihydrite with different degrees of crystallinity. *Environ. Sci. Technol.* **2023**, *57* (17), 6934−6943.
(15) Sheng, A.; Li, X.; Arai, Y.; Ding, Y.; Rosso, K. M.; Liu, J. Citrate controls Fe(II)-catalyzed transformation of ferrihydrite by complexation of the labile Fe(III) intermediate. *Environ. Sci. Technol.* **2020**, *54* (12), 7309−7319.
(16) Sheng, A.; Liu, J.; Li, X.; Luo, L.; Ding, Y.; Chen, C.; Zhang, X.; Wang, C.; Rosso, K. M. Labile Fe(III) supersaturation controls nucleation and properties of product phases from Fe(II)-catalyzed ferrihydrite transformation. *Geochim. Cosmochim. Acta* **2021**, *309*, 272−285.
(17) Handler, R. M.; Beard, B. L.; Johnson, C. M.; Scherer, M. M. Atom exchange between aqueous Fe(II) and goethite: an Fe isotope tracer study. *Environ. Sci. Technol.* **2009**, *43* (4), 1102−1107.
(18) Handler, R. M.; Frierdich, A. J.; Johnson, C. M.; Rosso, K. M.; Beard, B. L.; Wang, C.; Latta, D. E.; Neumann, A.; Pasakarnis, T.; Premaratne, W. A. P. J.; et al. Fe(II)-catalyzed recrystallization of goethite revisited. *Environ. Sci. Technol.* **2014**, *48* (19), 11302−11311.
(19) Joshi, P.; Fantle, M. S.; Larese-Casanova, P.; Gorski, C. A. Susceptibility of goethite to Fe^{2+}-catalyzed recrystallization over time. *Environ. Sci. Technol.* **2017**, *51* (20), 11681−11691.
(20) Joshi, P.; Gorski, C. A. Anisotropic morphological changes in goethite during Fe^{2+}-catalyzed recrystallization. *Environ. Sci. Technol.* **2016**, *50* (14), 7315−7324.
(21) Pedersen, H. D.; Postma, D.; Jakobsen, R.; Larsen, O. Fast transformation of iron oxyhydroxides by the catalytic action of aqueous Fe(II). *Geochim. Cosmochim. Acta* **2005**, *69* (16), 3967−3977.
(22) Gorski, C. A.; Handler, R. M.; Beard, B. L.; Pasakarnis, T.; Johnson, C. M.; Scherer, M. M. Fe atom exchange between aqueous Fe^{2+} and magnetite. *Environ. Sci. Technol.* **2012**, *46* (22), 12399−12407.
(23) Rosso, K. M.; Yanina, S. V.; Gorski, C. A.; Larese-Casanova, P.; Scherer, M. M. Connecting observations of hematite (α-Fe_2O_3) growth catalyzed by Fe(II). *Environ. Sci. Technol.* **2010**, *44* (1), 61−67.
(24) Yanina, S. V.; Rosso, K. M. Linked reactivity at mineral-water interfaces through bulk crystal conduction. *Science* **2008**, *320* (5873), 218−222.
(25) Joshi, P.; Fantle, M. S.; Boualavong, J.; Gorski, C. A. Quantifying the rate of Fe2+-catalyzed recrystallization based on a unifying model framework. *Geochim. Cosmochim. Acta* **2022**, *336*, 423−435.
(26) Gorski, C. A.; Fantle, M. S. Stable mineral recrystallization in low temperature aqueous systems: A critical review. *Geochim. Cosmochim. Acta* **2017**, *198*, 439−465.
(27) Frierdich, A. J.; Beard, B. L.; Rosso, K. M.; Scherer, M. M.; Spicuzza, M. J.; Valley, J. W.; Johnson, C. M. Low temperature, non-stoichiometric oxygen-isotope exchange coupled to Fe(II)−goethite interactions. *Geochim. Cosmochim. Acta* **2015**, *160*, 38−54.
(28) Taylor, S. D.; Liu, J.; Zhang, X.; Arey, B. W.; Kovarik, L.; Schreiber, D. K.; Perea, D. E.; Rosso, K. M. Visualizing the iron atom exchange front in the Fe(II)-catalyzed recrystallization of goethite by atom probe tomography. *Proc. Natl. Acad. Sci. U.S.A.* **2019**, *116* (8), 2866−2874.
(29) Frierdich, A. J.; Saxey, D. W.; Adineh, V. R.; Fougerouse, D.; Reddy, S. M.; Rickard, W. D.; Sadek, A. Z.; Southall, S. C. Direct observation of nanoparticulate goethite recrystallization by atom probe analysis of isotopic tracers. *Environ. Sci. Technol.* **2019**, *53* (22), 13126−13135.
(30) Southall, S. C.; Micklethwaite, S.; Wilson, S.; Frierdich, A. J. Changes in crystallinity and tracer-isotope distribution of goethite during Fe(II)-accelerated recrystallization. *ACS Earth Space Chem.* **2018**, *2* (12), 1271−1282.
(31) Frierdich, A. J.; Beard, B. L.; Reddy, T. R.; Scherer, M. M.; Johnson, C. M. Iron isotope fractionation between aqueous Fe(II) and goethite revisited: New insights based on a multi-direction approach to equilibrium and isotopic exchange rate modification. *Geochim. Cosmochim. Acta* **2014**, *139*, 383−398.
(32) Williams, A. G.; Scherer, M. M. Spectroscopic evidence for Fe(II)-Fe(III) electron transfer at the iron oxide- water interface. *Environ. Sci. Technol.* **2004**, *38* (18), 4782−4790.
(33) Qafoku, O.; Kovarik, L.; Bowden, M. E.; Nakouzi, E.; Sheng, A.; Liu, J.; Pearce, C. I.; Rosso, K. M. Nanoscale observations of Fe (II)-induced ferrihydrite transformation. *Environ. Sci. Nano* **2020**, *7* (10), 2953−2967.
(34) Notini, L.; ThomasArrigo, L. K.; Kaegi, R.; Kretzschmar, R. Coexisting goethite promotes Fe (II)-catalyzed transformation of ferrihydrite to goethite. *Environ. Sci. Technol.* **2022**, *56* (17), 12723−12733.
(35) Burleson, D. J.; Penn, R. L. Two-step growth of goethite from ferrihydrite. *Langmuir* **2006**, *22* (1), 402−409.
(36) Jang, J.-H.; Mathur, R.; Liermann, L. J.; Ruebush, S.; Brantley, S. L. An iron isotope signature related to electron transfer between aqueous ferrous iron and goethite. *Chem. Geol.* **2008**, *250* (1−4), 40−48.
(37) Sidhu, P.; Gilkes, R.; Cornell, R.; Posner, A.; Quirk, J. Dissolution of iron oxides and oxyhydroxides in hydrochloric and perchloric acids. *Clays Clay Miner.* **1981**, *29*, 269−276.
(38) Zachara, J. M.; Fredrickson, J. K.; Smith, S. C.; Gassman, P. L. Solubilization of Fe (III) oxide-bound trace metals by a dissimilatory Fe (III) reducing bacterium. *Geochim. Cosmochim. Acta* **2001**, *65* (1), 75−93.
(39) Stookey, L. L. Ferrozine—a new spectrophotometric reagent for iron. *Anal. Chem.* **1970**, *42* (7), 779−781.
(40) Xia, Q.; Jin, Q.; Chen, Y.; Zhang, L.; Li, X.; He, S.; Guo, D.; Liu, J.; Dong, H. Combined effects of Fe(III)-bearing nontronite and organic ligands on biogenic U(IV) oxidation. *Environ. Sci. Technol.* **2022**, *56* (3), 1983−1993.
(41) Pan, Z.; Roebbert, Y.; Beck, A.; Bartova, B.; Vitova, T.; Weyer, S.; Bernier-Latmani, R. Persistence of the isotopic signature of pentavalent uranium in magnetite. *Environ. Sci. Technol.* **2022**, *56* (3), 1753−1762.
(42) Collins, R. N.; Rosso, K. M. Mechanisms and rates of U(VI) reduction by Fe(II) in homogeneous aqueous solution and the role of U(V) disproportionation. *J. Phys. Chem. A* **2017**, *121* (35), 6603−6613.
(43) Fantle, M. S.; Tipper, E. T. Calcium isotopes in the global biogeochemical Ca cycle: Implications for development of a Ca isotope proxy. *Earth Sci. Rev.* **2014**, *129*, 148−177.
(44) Scrucca, L. GA: A package for genetic algorithms in R. *J. Stat. Softw.* **2013**, *53*, 1−37.
(45) Scrucca, L. On some extensions to GA package: hybrid optimization, parallelisation and islands evolution. *R J.* **2017**, *9* (1), 187−206.
(46) Jeon, B.-H.; Dempsey, B. A.; Burgos, W. D. Kinetics and mechanisms for reactions of Fe(II) with iron(III) oxides. *Environ. Sci. Technol.* **2003**, *37* (15), 3309−3315.
(47) Jeon, B.-H.; Dempsey, B. A.; Burgos, W. D.; Royer, R. A. Reactions of ferrous iron with hematite. *Colloids Surf., A* **2001**, *191* (1−2), 41−55.
(48) Peng, H.; Pearce, C. I.; Huang, W.; Zhu, Z.; N'Diaye, A. T.; Rosso, K. M.; Liu, J. Reversible Fe(II) uptake/release by magnetite nanoparticles. *Environ. Sci. Nano* **2018**, *5* (7), 1545−1555.
(49) Gorski, C. A.; Edwards, R.; Sander, M.; Hofstetter, T. B.; Stewart, S. M. Thermodynamic characterization of iron oxide−aqueous Fe^{2+} redox couples. *Environ. Sci. Technol.* **2016**, *50* (16), 8538−8547.

https://doi.org/10.1021/acs.est.5c11748
Environ. Sci. Technol. XXXX, XXX, XXX−XXX

(50) Taylor, S. D.; Liu, J.; Arey, B. W.; Schreiber, D. K.; Perea, D. E.; Rosso, K. M. Resolving iron(II) sorption and oxidative growth on hematite (001) using atom probe tomography. *J. Phys. Chem. C* **2018**, *122* (7), 3903−3914.
(51) Beard, B. L.; Handler, R. M.; Scherer, M. M.; Wu, L.; Czaja, A. D.; Heimann, A.; Johnson, C. M. Iron isotope fractionation between aqueous ferrous iron and goethite. *Earth Planet. Sci. Lett.* **2010**, *295* (1−2), 241−250.
(52) Asael, D.; Tissot, F. L.; Reinhard, C. T.; Rouxel, O.; Dauphas, N.; Lyons, T. W.; Ponzevera, E.; Liorzou, C.; Chéron, S. Coupled molybdenum, iron and uranium stable isotopes as oceanic paleoredox proxies during the Paleoproterozoic Shunga Event. *Chem. Geol.* **2013**, *362*, 193−210.
(53) Beard, B. L.; Johnson, C. M.; Cox, L.; Sun, H.; Nealson, K. H.; Aguilar, C. Iron isotope biosignatures. *Science* **1999**, *285* (5435), 1889−1892.
(54) Johnson, C. M.; Beard, B. L.; Roden, E. E. The iron isotope fingerprints of redox and biogeochemical cycling in modern and ancient Earth. *Annu. Rev. Earth Planet. Sci.* **2008**, *36* (1), 457−493.

https://doi.org/10.1021/acs.est.5c11748
Environ. Sci. Technol. XXXX, XXX, XXX−XXX